Nonlinear Optical Crystal $Y_xLa_ySc_z(BO_3)_4$ ($x + y + z = 4$)

Ning Ye,[†,§] Jennifer L. Stone-Sundberg,[†] Michael A. Hruschka,[†] Gerard Aka,[‡] Wei Kong,[†] and Douglas A. Keszler*[,†]

Department of Chemistry, Gilbert Hall 153, Oregon State University, Corvallis, Oregon 97331-4003, Ecole Nationale Supérieure de Chimie de Paris, 11, rue Pierre et Marie Curie, 75231 Paris Cedex 05, France, and Fujian Institute of Research on the Structure of Matter, Chinese Academy of Sciences, Fuzhou, Fujian 350002, P. R. China

Received January 14, 2005. Revised Manuscript Received February 18, 2005

The new nonlinear optical crystal $Y_xLa_ySc_z(BO_3)_4$ ($x + y + z = 4$) has been discovered. Phase boundaries have been established in the determination of the *x*, *y*, *z* composition parameters that define the existence region of the trigonal huntite-type structure. From single-crystal X-ray diffraction measurements, the member $Y_{0.57}La_{0.72}Sc_{2.71}(BO_3)_4$ has been found to crystallize in space group *R*32 with cell dimensions $a = 9.774(1)$ and $c = 7.944(3)$ Å. Large single crystals have been grown by a high-temperature solution method. The high-energy optical absorption edge for polished pieces was found to be at a wavelength shorter than 200 nm. Sellmeier equations for the dispersion in the refractive indices were determined on the basis of curve fitting of data obtained by the method of minimum deviation. From modeling and optical measurements on powders, the nonlinear optical coefficient d_{11} has been determined to be 1.4 pm/V.

Introduction

The structural, optical, and crystal-growth properties of the trigonal huntite derivative $YAl_3(BO_3)_4$ (YAB) have been extensively studied during the past four decades.[1] Interest in this material arises from its high frequency-conversion efficiency and ability to substitutionally accept lanthanide laser-active ions on the Y site. The major impediment, however, in developing the compound for applications has been the difficulty in growing large, high-quality crystals. At present, the best known flux for the growth of YAB is a complex polymolybdate,[2] which suffers from a relatively high volatility and incorporation of Mo into the crystals; the latter problem leads to a near UV absorption band that limits numerous potential applications at short wavelengths.

To circumvent these crystal-growth problems, efforts have been directed to the development of the related Sc huntite derivatives $LnSc_3(BO_3)_4$ (Ln = lanthanide).[3] These materials exist in the noncentrosymmetric trigonal huntite structure of YAB for some lighter lanthanides, e.g., $CeSc_3(BO_3)_4$,[4] while the transparent La derivative, $LaSc_3(BO_3)_4$ (LSB),[5] crystallizes in monoclinic variants of the huntite structure. Although a trigonal phase of LSB has been reported,[6] this result has not been reproduced by us and others.[7] Nevertheless, the monoclinic structure of LSB can be converted to the trigonal form by doping with a smaller lanthanide, e.g., $La_{1-x}Nd_xSc_3(BO_3)_4$,[7] undergoing alterations in structure over selected doping levels similar to those in the $Y_{1-x}Nd_xAl_3(BO_3)_4$ (NYAB) system.[8] To form a trigonal phase from LSB, an appropriate size ratio of *r*(Ln)/*r*(Sc) must be satisfied, i.e., this ratio must be smaller than that observed in LSB. To realize transparency at short wavelengths while retaining the desirable nonlinear properties of the trigonal phase, we have substituted Y for La and Sc in LSB to achieve this size tuning. The resulting trigonal phase is amenable to crystal growth, yielding transparent, high-quality crystals. In this contribution, we describe the crystal structure, phase relations, and optical properties of the first example of a trigonal borate huntite with transparency in the deep UV—the promising nonlinear optical crystal $Y_xLa_ySc_z(BO_3)_4$ ($x + y + z = 4$), which we refer to as YLSB.

Experimental Section

Powder samples of YLSB were prepared by reacting stoichiometric ratios of La_2O_3 (Stanford Materials, 99.999%), Y_2O_3 (Stanford Materials, 99.999%), Sc_2O_3 (Stanford Materials, 99.99%), and B_2O_3 (Cerac, 99.95%). $LiBO_2$ (5 wt %, Cerac, 99.9%) was added to promote the reaction; this fluxing agent was later removed by washing the product in H_2O. The samples were ground and

* To whom correspondence should be addressed. Phone: 541-737-6736. Fax: 541-737-2062. E-mail: douglas.keszler@oregonstate.edu.
† Oregon State University.
‡ Ecole Nationale Supérieure de Chimie de Paris.
§ Fujian Institute of Research on the Structure of Matter.

(1) (a) Mills, A. D. *Inorg. Chem.* **1962**, *1*, 960. (b) Ballman, A. A. *Am. Mineral.* **1962**, *47*, 138. (c) Liao, J. Y.; Lin, Y.; Chen, Z.; Luo, Y.; Huang, Y. *J. Cryst. Growth* **2004**, *267*, 134. (d) Aka, G.; Viegas, N.; Teisseire, B.; Kahn-Harari, A.; Godard, J. *J. Mater. Chem.* **1995**, *5*, 58.
(2) Leonyuk, N. I.; Leonyuk, L. I. *Prog. Cryst. Growth Charact.* **1995**, *31*, 179.
(3) Kutovoi, S. A.; Laptev, V. V.; Matsnev, S. Y. *Sov. J. Quantum Electron.* **1991**, *21*, 131.
(4) Peterson, G. A.; Keszler, D. A.; Thomas, T. A. *Int. J. Inorg. Mater.* **2000**, *2*, 101.
(5) (a) Sun, H. Ph. D. dissertation, Oregon State University, Corvallis, OR, 1989. (b) Meyn, J. P.; Jensen, T.; Huber, G. *IEEE J. Quantum Electron.* **1994**, *30*, 913.
(6) He, M.; Wang, G.; Lin, Z.; Chen, W.; Lu, S.; Wu, Q. *Mater. Res. Innovations* **1999**, *2*, 345.
(7) Li, Y.; Aka, G.; Kahn-Harari, A.; Vivien, D. *J. Mater. Res.* **2001**, *16*, 38.
(8) Jung, S. T.; Yoon, J. T.; Chung, S. J. *Mater. Res. Bull.* **1996**, *31*, 1022.

10.1021/cm050090c CCC: $30.25
Published on Web 04/15/2005

Table 1. ICP Elemental Analysis and Stoichiometry for YLSB

element	solution concn (ppm)	no. per formula unit
B		4[a]
O		12[a]
Sc	1.98	2.71[b]
Y	0.82	0.57[b]
La	1.63	0.72[b]

[a] Assuming 20 atoms total per formula unit. [b] Assuming $x + y + z = 4$; $Y_xLa_ySc_z(BO_3)_4$.

heated in Pt crucibles at 850 °C for 2 h and 1100 °C for 12 h; the samples were additionally ground after the heat treatment at 850 °C.

Crystals of approximate composition $Y_{0.57}La_{0.72}Sc_{2.71}(BO_3)_4$ were grown by using the flux $3Li_2O{\cdot}2B_2O_3$ (Li_2CO_3, Cerac, 99.9%; B_2O_3, Cerac, 99.9%); the composition of the mixture for crystal growth was 0.6:0.35:1.5:7:7.5 $Y_2O_3/La_2O_3/Sc_2O_3/B_2O_3/Li_2O$. This mixture was heated in a Pt crucible to 1050 °C and held at this temperature for 2 days. A seed with orientation [$11\bar{2}0$] was attached with Pt wire to an alumina rod and then suspended in the melt to determine the crystallization temperature and initiate growth. Crystals were grown by cooling at a rate of 2 °C/day, continuing until the desired boule size was obtained. The flux attached to the crystal was readily dissolved in nitric acid.

A differential thermal analysis scan was obtained on a TA Instruments Thermal Analysis system. The sample was heated and cooled at 10 °C/min.

Elemental analysis of a selected YLSB crystal was performed by using a JY-2000 inductively coupled plasma optical emission spectrometer (ICP−OES) and Sepex Certiprep standards. The crystal samples were first melted with $LiBO_2$ in Pt crucibles at 1100 °C and subsequently dissolved in nitric acid. The solutions were prepared with concentrations below 5000 ng/mL.

X-ray Measurements. X-ray diffraction patterns of the polycrystalline materials were obtained on a Siemens D5000 diffractometer by using Cu Kα radiation. Single-crystal X-ray diffraction data were obtained at room temperature on a Rigaku AFC6R diffractometer with monochromatic Mo Kα radiation ($\lambda = 0.71073$ Å). A transparent block of YLSB having dimensions 0.1 × 0.07 × 0.05 mm was fractured from a large boule and mounted on a glass fiber with epoxy for structure determination. Cell constants and the orientation matrix for data collection were obtained from a least-squares refinement with 25 automatically centered reflections in the range $25° < 2\theta < 35°$; no decay in intensity was noted during data collection. The structure was solved by using the computer program SHELXL-97 and then refined by using a full-matrix least-squares refinement on F^2 with the program SHELXL-97[9] as programmed in the software suite WinGX v1.64.03.[10] Crystal data and refinement summaries are given in Table 2. Final atomic coordinates and equivalent isotropic displacement parameters are listed in Table 3. Occupancy factors for the La and Sc sites were fixed to the values that were determined by ICP elemental analysis, as deviations from these occupancies afforded increased residuals in the least-squares refinements.

Optical Measurements. The experimental method of Kurtz and Perry[11] was used to measure powder SHG signals with a 1064-nm laser. The sample was ground and sieved by using a series of mesh sizes in the range of 25−250 μm. A sample of β-BaB_2O_4 was prepared as a reference material in an identical fashion. The samples were pressed between glass microscope cover slides and secured with tape in 1-mm thick aluminum holders containing a 5-mm diameter hole. They were then placed in a light-tight box and excited with 20-mJ, 1064-nm pulses from a Q-switched New Wave Research Minilase-20 Nd:YAG laser. A cutoff filter was used to limit background flash-lamp light on the sample, and an interference filter (530 ± 10 nm) was used to select the second harmonic for detection with a photomultiplier tube attached to a Tektronix SC 504 80-MHz oscilloscope.

The transmittance spectrum was recorded at room temperature by using a 1.53-mm-thick slab of YLSB polished on both sides and a Bruins Omega 10 spectrophotometer with a range of 190−1800 nm. Refractive indices were measured over the wavelength range of 4678.2−9638.2 Å by using the minimum-deviation method and a YLSB prism oriented with the crystallographic *c* axis parallel to the prism axis. Selected phase-matching angles were measured with a dye laser.

Table 2. Crystal Data and Structure Refinement for $Y_{0.57}La_{0.72}Sc_{2.71}(BO_3)_4$[a]

formula	$Y_{0.57}La_{0.72}Sc_{2.71}(BO_3)_4$
formula mass	507.78 amu
temperature	290(2) K
wavelength	0.71073 Å
space group	*R*32
a	9.774(1) Å
c	7.946(2) Å
cell volume	657.4(2) Å^3
Z	3
density (calcd)	3.848 g/cm^3
absorption coefficient	9.257 mm^{-1}
F(000)	709
crystal size	0.1 × 0.07 × 0.05 mm^3
θ range for data collection	3.52−30.04°
index range	$-13 \le h \le 13$, $-13 \le k \le 13$, $-11 \le l \le 11$
reflections collected	2574
independent reflections	437
reflection with $I > 2\sigma(I)$	437
completeness to $\theta = 30.0°$	100%
absorption correction	none
refinement method	full-matrix least squares on F^2
data/restraints/parameters	437/0/35
goodness-of-fit on F^2	1.081
R ($I > 2\sigma$ (I))	0.0296
R/wR (all data)	0.0296/0.0815
largest diff. peaks	+0.889 and −1.353 e/Å^{-3}

[a] Complete crystal-structure results may be obtained from Fachinformationzentrum Karlsruhe GmbH, Hermann von Helmholtz Platz 1, Leopolschafen (Germany); depository number CSD-391262.

Results and Discussion

A differential thermal analysis (DTA) trace for the composition $La_{0.7}Y_{0.3}Sc_3(BO_3)_4$ exhibits a broad melting event beginning at 1220 and ending near 1475 °C. On cooling, a sharp exotherm is observed at 1218 °C. In principle, a solid solution such as $La_xY_{1-x}Sc_3(BO_3)_4$ ($x > 0$) will not exhibit congruent melting and a sharp endotherm on heating. The DTA trace is consistent with this behavior, and a flux must be used to grow crystals. Hence, colorless and transparent YLSB crystals of composition $Y_{0.57}La_{0.72}Sc_{2.71}(BO_3)_4$ and dimensions near 30 × 30 × 10 mm (Figure 1) have been grown by a high-temperature top-seeded solution method. The crystals have the typical morphology of the huntite series,[2] clearly exhibiting {$11\bar{2}0$} and {$10\bar{1}1$} facets. They are chemically stable with respect to water and strong acid, and they are mechanically robust and sufficiently hard to be readily polished.

The structure of YLSB is illustrated in Figure 2. It is a classical huntite type with nearly planar layers of BO_3 groups

(9) Sheldrick, G. M. SHELXS-97 − A program for automatic solution of crystal structure refinement; Release 97−2; 1997.
(10) Farrugia, L. J. *J. Appl. Crystallogr*. **1999**, *32*, 837.
(11) Kurtz, S. K. Perry, T. T. *J. Appl. Phys.* **1968**, *39* (8), 3798.

Table 3. Atomic Positions and Isotropic Displacement Factors for $Y_{0.57}La_{0.72}Sc_{2.71}(BO_3)_4$

atom	*x*	*y*	*z*	Wyckoff	U_{eq} (Å^2) × 10^3	occupancy
La	0	0	0	3*a*	10.9(3)	0.72
Y(1)	0	0	0	3*a*	10.9(3)	0.28
Sc	−0.1199(2)	2/3	2/3	9*d*	11.1(3)	0.9
Y(2)	−0.1199(2)	2/3	2/3	9*d*	11.1(3)	0.1
B(1)	−0.217(1)	2/3	1/6	9*e*	12(1)	1
B(2)	0	0	1/2	3*b*	10(2)	1
O(1)	0	−0.4086(8)	1/2	9*e*	23(2)	1
O(2)	−0.0188(6)	0.1927(6)	−0.1809(5)	18*f*	16.1(8)	1
O(3)	0	−0.1402(6)	1/2	9*e*	12(1)	1

Table 4. Compositions with Trigonal Huntite Structure

	$(Y_{x'}La_{1-x'})_{tri}(Y_{y'}Sc_{3-y'})_{octa}(BO_3)_4$		
composition	*x*′	*y*′	cell volume (Å^3)
$Y_{0.28}La_{0.77}Sc_{2.95}(BO_3)_4$	0.23	0.05	666.35(9)
$Y_{0.32}La_{0.76}Sc_{2.92}(BO_3)_4$	0.24	0.08	666.6(1)
$Y_{0.38}La_{0.80}Sc_{2.82}(BO_3)_4$	0.20	0.18	670.56(1)
$Y_{0.42}La_{0.73}Sc_{2.85}(BO_3)_4$	0.27	0.15	667.51(5)
$Y_{0.47}La_{0.75}Sc_{2.78}(BO_3)_4$	0.25	0.22	670.5(1)

extending in the *ab* plane. The La, Y, and Sc atoms occupy 6-coordinate sites between these layers with the Y and La atoms centering a distorted trigonal prism and Y and Sc atoms residing in a distorted octahedron. The trigonal prisms are completely isolated one from the other, while the Sc-(Y)O_6 octahedra share edges. Connectivities between the dissimilar polyhedra occur only through vertex sharing.

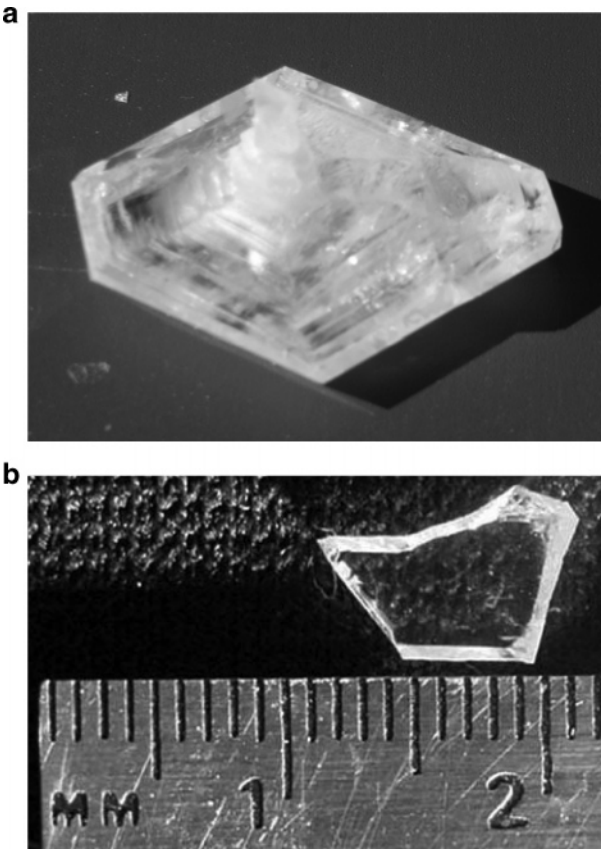

Figure 1. (a) As-grown $Y_{0.57}La_{0.72}Sc_{2.71}(BO_3)_4$ crystal; dimensions are 30 × 30 × 10 mm; and (b) polished fragment of YLSB.

The summary of ICP elemental analysis of a YLSB crystal, assuming stoichiometric amounts of B, is given in Table 1. The stoichiometry was calculated on the basis of 12 O atoms and 4 B atoms in each formula unit, consistent with the composition of members of the huntite family. The crystal is deficient in Sc, indicating Y atoms partially occupy the Sc site.

To better define the stability region for the trigonal phase, forty samples were prepared with a synthesis temperature of 1100 °C on the basis of the formula $Y_xLa_ySc_z(BO_3)_4$ ($x + y + z = 4$); product phases were identified by using X-ray powder diffraction. All results are displayed in a quasi-ternary phase diagram (Figure 3) with the three end members YBO_3,

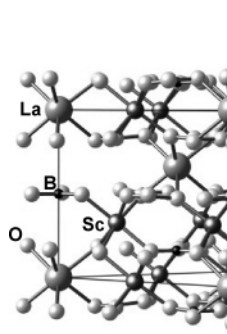

Figure 2. Crystal structure of YLSB.

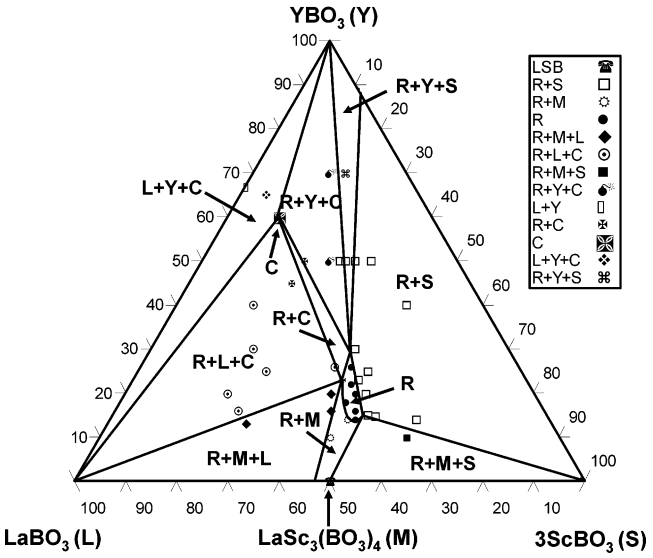

Figure 3. Quasi-ternary phase diagram of $LaBO_3$−YBO_3−$ScBO_3$ system; R = trigonal YLSB phase and C = calcite-type phase.

$LaBO_3$, and $ScBO_3$. LSB was found to be monoclinic at 1100 °C, and it is the only phase on the quasi-binary line between the end members $LaBO_3$ and $ScBO_3$. Two single phases were found inside the triangle—a calcite phase (C) near the composition $Y_2LaSc(BO_3)_4$ and a trigonal phase (R) covering the composition range of $0.29 < x < 0.67$, $0.67 < y < 0.82$, and $2.64 < z < 3.00$. The latter phase was proven to be a trigonal-huntite derivative on the basis of the single-crystal structure determination. Phase boundaries, as determined from interpretation of the diffraction patterns, are indicated in the diagram, cf., Figure 3.

Selected compositions for samples within the trigonal-huntite region of the phase diagram are listed in Table 4. For the general formula $Y_xLa_ySc_z(BO_3)_4$, Y atoms replace not only the La atoms in the trigonal prisms but also the Sc atoms in the octahedra. This result can be appreciated by comparing cell volumes for the compositions $Y_{0.28}La_{0.77}Sc_{2.95}(BO_3)_4$ and $Y_{0.47}La_{0.75}Sc_{2.78}(BO_3)_4$. While the La concentrations in these two compositions are similar, the higher Y concentration of $Y_{0.47}La_{0.75}Sc_{2.78}(BO_3)_4$ relative to $Y_{0.28}La_{0.77}Sc_{2.95}(BO_3)_4$ leads to a 0.6% increase in cell volume, which can only occur if the Y atom substitutes on the small Sc site.

The formula for demonstrating Y-atom substitution in YLSB can be written as $(Y_{x'}La_{1-x'})_{tri}(Y_{y'}Sc_{3-y'})_{octa}(BO_3)_4$. The sizes of the trigonal prisms and the octahedra required to form the huntite structure are achieved by maintaining the suitable Y atom doping level in each site. In general, the unit-cell volume varies with the sizes of both the trigonal prism and the octahedron. This can be expressed in the following equations by using atomic radii (R)[12] and appropriately weighted occupancies for the Y, La, and Sc atoms.

$$V \propto R_Y^3 \cdot x' + R_{La}^3 \cdot (1 - x') + R_Y^3 \cdot y' + R_{Sc}^3 \cdot (3 - y')$$

$$V \propto R_{La}^3 + 3R_{Sc}^3 + (R_Y^3 - R_{La}^3)x' + (R_Y^3 - R_{Sc}^3)y'$$

If the Y atoms are distributed over both the La and Sc sites, the points in a three-dimensional plot of V, x', and y' should occupy a plane. By defining the effective concentration, C_{eff}, the results can be projected onto a two-dimensional plot of V vs C_{eff}.

$$C_{eff} = -\frac{(R_Y^3 - R_{La}^3)x' + (R_Y^3 - R_{Sc}^3)y'}{\sqrt{(R_Y^3 - R_{La}^3)^2 + (R_Y^3 - R_{Sc}^3)^2}}$$

$$V \propto R_{La}^3 + 3R_{Sc}^3 + \sqrt{(R_Y^3 - R_{La}^3)^2 + (R_Y^3 - R_{Sc}^3)^2} \cdot C_{eff}$$

As seen from the linear relationship between C_{eff} and V in Figure 4, the Y atoms do indeed appear to be distributed across both sites.

As shown in Figure 5, the crystals exhibit high transparency in the UV portion of the spectrum. In our measurement, the short-wavelength transmission cutoff extends to approximately 193 nm, opening a wide window for UV applications. It should be noted, however, that this cutoff wavelength is very close to the measurement limit of the spectrophotometer.

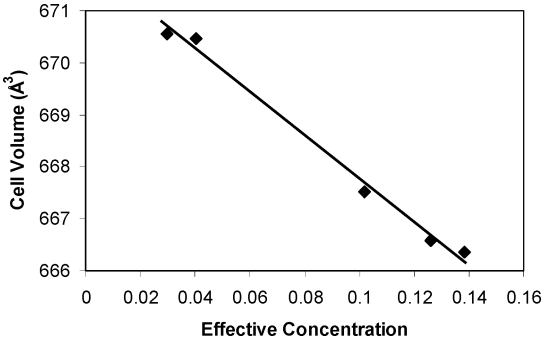

Figure 4. Relationship between effective concentration, C_{eff}, and cell volume, V.

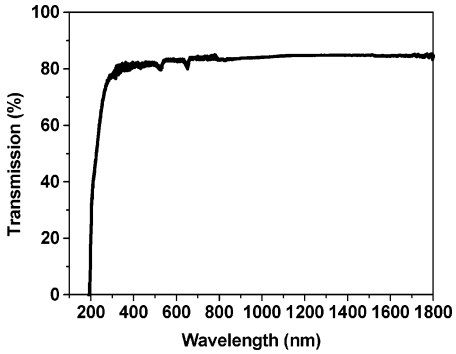

Figure 5. Transmittance curve of YLSB crystal.

Table 5. Refractive Indices for $Y_{0.57}La_{0.72}Sc_{2.71}(BO_3)_4$ Crystal

wavelength (μm)	n_o		n_e	
	exp.	calc.	exp.	calc.
0.40466	1.87557	1.87566	1.78609	1.78626
0.4047	1.87578	1.87564	1.78639	1.78625
0.40778	1.87444	1.87466	1.78526	1.78543
0.4358	1.86679	1.86674	1.77884	1.77890
0.43584	1.86663	1.86673	1.77884	1.77889
0.45554	1.86230	1.86213	1.77541	1.77508
0.45932	1.86137	1.86132	1.77449	1.77441
0.46782	1.85949	1.85958	1.77323	1.77297
0.46801	1.85978	1.85954	1.77295	1.77294
0.47222	1.85811	1.85872	1.77217	1.77226
0.47999	1.85733	1.85726	1.77113	1.77105
0.48105	1.85803	1.85707	1.77088	1.77089
0.50858	1.85236	1.85251	1.76712	1.76712
0.50858	1.85252	1.85251	1.76721	1.76712
0.54607	1.84737	1.84744	1.76279	1.76295
0.5461	1.84740	1.84744	1.76319	1.76294
0.57696	1.84389	1.84402	1.75997	1.76014
0.578	1.84386	1.84392	1.76003	1.76006
0.57906	1.84368	1.84381	1.75967	1.75997
0.5893	1.84246	1.84281	1.75878	1.75915
0.63623	1.83870	1.83882	1.75573	1.75593
0.77359	1.83131	1.83091	1.75028	1.74979
0.82437	1.82909	1.82885	1.74857	1.74829
0.87777	1.82711	1.82700	1.74718	1.74700
0.93424	1.82518	1.82530	1.74567	1.74589
0.96381	1.82429	1.82450	1.74518	1.74539

The refractive indices at 26 wavelengths covering visible and near-infrared wavelengths were determined with the minimum-deviation method (Table 5). The indices were fit to the Sellmeier equations

$$n_o^2 = 3.30760 + \frac{0.03027}{\lambda^2 - 0.02139} - 0.01309\lambda^2$$

$$n_e^2 = 3.01746 + \frac{0.02530}{\lambda^2 - 0.01755} + 0.00125\lambda^2$$

(12) Shannon, R. D. *Acta Crystallogr., Sect. A: Found. Crystallogr.* **1976**, *32*, 751.

Table 6. Parameters for Selected Wave Mixing with $Y_{0.57}La_{0.72}Sc_{2.71}(BO_3)_4$ Crystal (Parameters for the Nonlinear Crystals β-BaB_2O_4 and LiB_3O_5 Are Sequentially Listed in Parentheses)[a]

wavelength (nm)	phase matching angle, θ_{pm} (deg)	effective nonlinear coefficient, d_{eff} (pm/V)	walk-off angle, ρ (deg)	acceptance angle, $\Delta\theta$ (mrad-cm)
1064 → 532	33.5	1.20	2.52	1.21
	(22.8, 11.4*)	(1.45, 1.00)	(3.19, 0.40)	(0.96, 7.53*)
750 → 375	49.7	0.90	2.78	0.77
	(31.2, 37.1*)	(1.34, 0.81)	(4.08, 1.03)	(0.53, 2.06*)
800 → 400	45.6	0.98	2.80	0.82
	(29.2, 31.7*)	(1.37, 0.86)	(3.89, 0.95)	(0.59, 2.39*)
900 → 450	39.7	1.10	2.72	0.95
	(26.1, 22.9*)	(1.41, 0.94)	(3.57, 0.75)	(0.72, 3.40*)
1064+532 → 355	49.9	0.90	2.82	0.71
	(31.3, 37.3*)	(1.33, 0.80)	(4.13, 1.05)	(0.49, 1.90*)
1064+514 → 347	51.1	0.87	2.80	0.70
	(31.9, 38.9*)	(1.32, 0.78)	(4.19, 1.07)	(0.47, 1.82*)
1064+355 → 266	72.9	0.39	1.77	0.84
	(40.3, 61.0*)	(1.16, 0.48)	(4.94, 1.01)	(0.30, 1.47*)
2100+213 → 193	64.2	0.55	4.04	0.23
	(40.7, 57.3*)	(1.14, 0.53)	(6.43, 1.42)	(0.15, 0.71)

[a] Asterisk (*) indicates angles for ϕ.

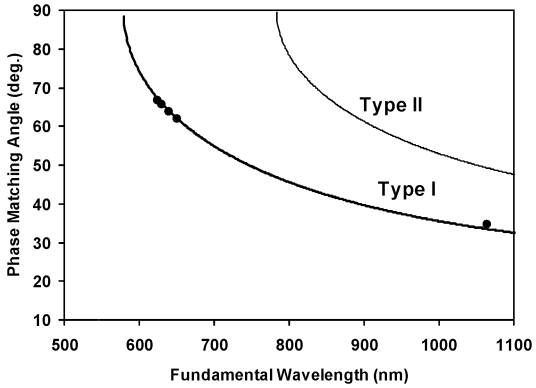

Figure 6. Calculated phase matching curves for second harmonic generation. Points represent measured values.

where n_o and n_e are the refractive indices for ordinary and extraordinary polarizations, respectively, and λ is the wavelength expressed in micrometers. YLSB is a negative uniaxial optical crystal, and the birefringence value ($\Delta n = n_o - n_e$) is approximately 0.085 over the measured wavelength region. This birefringence is consistent with the anisotropic nature of the crystal structure and the presence of layers of flat BO_3 groups.

On the basis of the Sellmeier equations, the phase-matching curves for second-harmonic generation (SHG) can be calculated for type-I and type-II phase matching, respectively (Figure 6). The shortest wavelength for type-I second-harmonic generation is predicted to be 290 nm from the calculated phase matching curves (Figure 6), and the phase matching angle for type-I second harmonic generation at 532 nm is 33.5°. Some phase-matching angles (θ_{pm}) at selected wavelengths were verified by measurements with a dye laser; the results were found to be consistent with calculated values (Figure 6).

The effective SHG coefficient d_{eff} is given by

$$d_{eff}^{type-I} = d_{11}\cos\theta\cos 3\phi$$

$$d_{eff}^{type-II} = d_{11}\cos^2\theta\sin 3\phi$$

YLSB has point-group symmetry D_3, so it has only one nonzero independent SHG coefficient, i.e., d_{11}, assuming

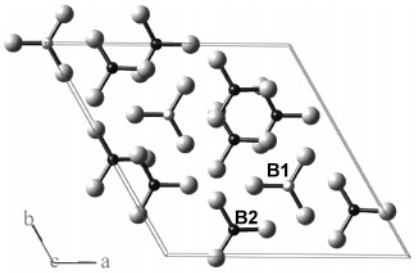

Figure 7. YLSB structure: view down the *c*-axis. Lightly shaded circles represent B(1) atoms, and heavily shaded circles represent B(2) atoms.

Kleinman symmetry relations. The magnitude of the coefficient d_{11} can be calculated on the basis of Anionic Group Theory by using the equation[13]

$$d_{11} = \frac{L^3}{V}\sum_{p=1}^{N}\sum_{ijk} R_{1i}R_{1j}R_{1k}\beta_{lmn}$$

where L is the local-field factor,[14] V is the unit-cell volume, R_{1x} is the orientation direction cosine for each BO_3 group, and β_{lmn} is the component of the hyperpolarizabilty tensor for each BO_3 group with the only nonzero component being β_{111}. As shown in Figure 7, there are twelve BO_3 groups in a unit cell; three are centered by atom B(1) (light) and nine are centered by atom B(2) (dark). The two types of groups are related by an approximate center of symmetry, so the sum of β_{lmn} according to the orientation (R) of individual groups is quite straightforward, i.e., $d_{11} \propto (9 - 3)/12 \times \beta_{111}$, i.e., the arrangement of BO_3 triangles in YLSB is 50% of optimum. The same BO_3 group arrangement is found in YAB, and its d_{11} coefficient has been reported to be 1.79 pm/V.[15] The d_{11} value for YLSB may then be deduced by comparing the number densities of BO_3 groups in YAB and YLSB as follows:

(13) Chen, C. T. *Development of New Nonlinear Optical Crystals in the Borate Series*; Harwood Academic Publishers: Langhorne, PA, 1993.
(14) Armstrong, J. A.; Bloembergen, N.; Ducuing, J.; Pershan, P. S. *Phys. Rev.* **1962**, *127* (6), 1918.
(15) Amano, S.; Mochizuki, T. *Nonlinear Opt.* **1991**, *1*, 297.

$$d_{11}(YLSB) = \frac{BO_3\ number\ group\ density\ (YLSB)}{BO_3\ number\ group\ density\ (YAB)} \times 1.79\ \text{pm/V}$$

From the number densities of 1.8×10^{22} and 2.2×10^{22} for YLSB and YAB, respectively, the predicted value of d_{11} for YLSB is 1.43 pm/V, assuming the same local-field corrections for the two materials. It is useful to note that considering the high number density of BO_3 groups in YAB (YLSB) and the demonstrated relationship between structure and nonlinear coefficient, the upper limit for the *d* coefficient for any highly transparent orthoborate crystal (cutoff $\lambda <$ 200 nm) can be predicted to be approximately 3 pm/V. Values greater than 1 pm/V certainly represent favorable group orientations and relatively high group number densities; they are also sufficient for many applications.

The second-harmonic signal produced by YLSB powders with a 1064-nm fundamental corresponds to $0.67 \times \beta$-BaB_2O_4 (BBO). These signals are proportional to the squares of the nonlinear *d* coefficients, assuming the phase-matching lengths for the two materials are the same. As a result, the ratio $d_{obs}(YLSB)/d_{obs}(BBO) = 0.8$. Since the reported *d* coefficient for β-BaB_2O_4 is 1.8 pm/V, the derived result for YLSB is 1.4 pm/V, a value in general agreement with the calculated value of 1.43 pm/V.

Parameters for some selected wave-mixing processes of practical interest for YLSB and the commercial materials BaB_2O_4 (BBO) and LiB_3O_5 (LBO) are given in Table 6. As seen from the table, many of the characteristics of YLSB are intermediate to those of BBO and LBO, as might be expected from consideration of its d_{11} value and birefringence, which fall between those of the other two crystals. Clearly, the high nonlinear coefficients, small walk-off angles, and relatively wide acceptance angles make YLSB a promising crystal for frequency conversion in the UV region.

Conclusions

A new nonlinear optical crystal $Y_xLa_ySc_z(BO_3)_4$ ($x + y + z = 4$) crystallizing in the trigonal huntite structure has been discovered. At the composition $Y_{0.57}La_{0.72}Sc_{2.71}(BO_3)_4$, it crystallizes in space group *R*32 with cell dimensions $a =$ 9.774(1) and $c = 7.944(3)$ Å. Phase equilibria have been examined in the system $LaBO_3-ScBO_3-YBO_3$, and the composition limits of the huntite-type solid solution have been established as $0.29 < x < 0.67$, $0.67 < y < 0.82$, and $2.64 < z < 3.00$. Crystals with approximate dimensions 30 $\times$ 30 $\times$ 10 mm have been grown by using a lithium-borate flux and a high-temperature top-seeded solution method. Linear and nonlinear optical properties were measured, indicating a wide transparency range extending into the deep UV ($\lambda <$ 200 nm), a moderate birefringence ($\Delta n = 0.085$), and a high second-order susceptibility coefficient ($d_{11} = 1.4$ pm/V). These features, coupled with higher chemical stability and mechanical durability relative to those of BBO and LBO, make YLSB a promising NLO material for practical applications.

Acknowledgment. This material is based upon work supported by Coherent Crystal Associates and the National Science Foundation under Grant ECS-0114017.

Supporting Information Available: X-ray crystallographic information file (CIF). This material is available free of charge via the Internet at http://pubs.acs.org.

CM050090C